Innovative Food Technologies 13(1) (2025) 23-35

Iranian Research Organization for Science and Technology (IROST)

Innovative Food Technologies

journal homepage: https://jift.irost.ir

Kinetic modeling of physicochemical changes in protein bars fortified with spirulina and phycocyanin during storage

Parnian Pourghasemian[a], Amir Pourfarzad[b,c]*, Aria Babakhani[d]

[a] MSc, Department of Food Science and Technology, Faculty of Agricultural Sciences, University of Guilan, Rasht, Iran.
[b] Associate Professor, Department of Chemical Technologies, Iranian Research Organization for Science & Technology (IROST), Tehran, Iran.
[c] Associate Professor, Department of Food Science and Technology, Faculty of Agricultural Sciences, University of Guilan, Rasht, Iran.
[d] Associate Professor, Fisheries Department, Faculty of Natural Resources, University of Guilan, Sowmeh Sara, Guilan, Iran.

ARTICLE INFO

Keywords:
Kinetic modelling,
Microalgae,
Oxidation,
Shelf life

ABSTRACT

Protein bars are widely recognized as popular health-oriented products; however, they are highly susceptible to physicochemical changes during storage, which may compromise consumer acceptance. One promising approach to minimize these undesirable effects is the use of natural compounds with strong antioxidant activity. Among them, the microalga *Spirulina platensis* stands out due to its richness in proteins, vitamins, and bioactive compounds, making it an attractive ingredient in the formulation of functional foods. Similarly, phycocyanin—a water-soluble protein pigment with remarkable antioxidant potential—has drawn attention for its ability to improve nutritional value and enhance oxidative stability. This study investigated the stability of protein bars fortified with spirulina and phycocyanin compared to a control formulation during 28 days of storage at room temperature, with evaluations carried out at 7-day intervals. Key parameters such as moisture content, water activity, acidity, peroxide value, and color difference (ΔE) were measured. To model the observed changes and determine the most suitable kinetic fit, statistical indicators including the coefficient of determination (R^2), chi-square (χ^2), mean bias error (MBE), and root mean square error (RMSE) were applied. The results demonstrated that fortification with spirulina and phycocyanin slowed down the rate of undesirable changes and improved the overall stability of the protein bars throughout storage. These findings highlight the promise of such natural ingredients in enhancing both the functionality and oxidative stability of protein bars, paving the way for the development of more sustainable and consumer-friendly health products.

1. Introduction

In recent years, increasingly busy lifestyles and time constraints have led many individuals to pay less attention to healthy dietary patterns. Skipping main meals has become a common behavior, with fast foods often serving as convenient replacements due to their ease of consumption and accessibility. However, such foods are typically high in calories, saturated fats, and other unhealthy components, and their frequent consumption is strongly associated with chronic conditions such as obesity and diabetes. In response to these concerns, the production and consumption of ready-to-eat nutritional products, such as food bars, have gained popularity as healthier alternatives to skipped meals. When formulated appropriately, these products can provide a balanced combination of macronutrients and essential micronutrients—particularly proteins and carbohydrates—thereby contributing to improved nutritional status [1,2].

Based on their composition and nutritional profile, nutritional bars are categorized into various groups, including energy bars, food bars, protein bars, and sports bars [3]. Some products, due to their composite formulation, may fall into more than one category [4]. Among these, protein bars occupy a prominent share of the market, largely because of their role in delivering high-quality protein, supporting muscle growth and maintenance, aiding post-exercise recovery, providing energy, and even contributing to weight management [5,6].

Protein bars are generally classified as intermediate-moisture foods, with reported water activity values ranging between 0.5 and 0.9 [7]. Maintaining their physicochemical and oxidative stability during storage—particularly at room temperature—remains a major challenge in the food industry. Factors such as moisture migration, changes in water activity, lipid oxidation, and color degradation can all contribute to product quality loss [5,8]. To address these challenges, the food industry has increasingly turned to natural antioxidant compounds to extend shelf life and preserve product quality [9].

Emerging research highlights the application of microalgae in improving both the nutritional and technological properties of food products. Reported benefits include emulsifying activity, enhanced color and flavor, improved stability, nutritional value, and extended shelf life [10]. Among microalgae, *Spirulina platensis*—a blue-green alga—is especially notable for

*Corresponding author email: amir.pourfarzad@gmail.com
DOI: http://dx.doi.org /10.22104/ift.2025.7810.2229
(Received: 09 August 2025, Received in revised form: 26 August 2025, Accepted: 06 September 2025)

its high content of proteins, essential fatty acids, vitamins, minerals, and antioxidant compounds, making it a valuable ingredient in the food and dietary supplements industries [11]. With rising global demand for protein sources, the production and utilization of spirulina have expanded considerably, as food companies explore diverse protein alternatives from animal, plant, microbial, and algal origins [12,13].

In addition to its nutritional richness, spirulina exhibits functional properties such as high water-binding capacity, gelling, and film-forming ability, which can enhance the technological performance of cereal-based products and improve their nutritional quality [14,15]. One of its key bioactive compounds is phycocyanin, a natural blue protein pigment with strong antioxidant, anti-inflammatory, anticancer, and immune-boosting properties. Recognized as safe, phycocyanin has been widely adopted as a natural substitute for synthetic dyes in foods and nutraceuticals [16-18].

Given the nutritional and functional attributes of spirulina and phycocyanin, their incorporation into novel health-oriented products—particularly in combination with carbohydrate- and fiber-rich sources such as brown rice flour—has attracted increasing attention. While numerous studies have focused on protein bar formulation, only a limited number have investigated the quality changes of these products during storage and their kinetic modeling. Monitoring kinetic changes in parameters such as moisture content, water activity, titratable acidity, peroxide value, and color difference (ΔE) can provide deeper insights into degradation patterns and product stability.

Therefore, the main objective of this study was to evaluate the physicochemical and oxidative changes of protein bars fortified with spirulina and phycocyanin during 28 days of storage at room temperature, and to model these changes using suitable mathematical approaches. The application of kinetic models in food quality analysis provides valuable insights for predicting shelf life, optimizing formulation design, selecting stabilizing agents, and determining suitable packaging and storage conditions. The findings of this research are expected to provide a scientific foundation for the development of stable, health-oriented protein bars in the food industry.

2. Materials and methods

2.1. Materials

The raw materials used in this study included brown rice flour (Giltaz Company, Iran), whey protein concentrate and starch powder (Roysa Online Store, Iran), food-grade glycerol (KLK, Malaysia), spirulina powder (Royaye Jalbek Pars Company, Iran), and phycocyanin powder (Zist Fanavaran Yakhteh Giti Sabz Company, Iran). Sunflower oil and distilled water were also used. The chemical reagents applied in analyses were phenolphthalein, sodium hydroxide, chloroform, sodium thiosulfate pentahydrate, and sodium carbonate (Merck Company, Germany); glacial acetic acid (Dr. Mojallali Company, Iran); and potassium iodide (Shimi Center store, Iran).

2.2. Methods

2.2.1. Preparation of protein bars

Protein bars were prepared using a cold-processing method at a controlled temperature of 25 °C to preserve the functional properties of heat-sensitive compounds. The formulation consisted of brown rice flour, whey protein concentrate, food-grade glycerol, sunflower oil, and distilled water (Table 1). Two types of samples were prepared: a control sample (without spirulina and phycocyanin) and a fortified sample containing spirulina and phycocyanin powders. The formulation of the fortified sample was based on the results of a previous optimization study [19] focusing on nutritional, structural, and sensory properties. First, spirulina and phycocyanin powders were thoroughly blended with the dry ingredients (brown rice flour and whey protein concentrate). The liquid components (glycerol, distilled water, and sunflower oil) were then gradually added and homogenized for 5 min at 50 rpm. The dough was molded into uniform silicone molds (2 × 2 × 2 cm) and stored in sealed polyethylene terephthalate (PET) containers at 25 °C for 28 days to reach moisture equilibrium before further analyses [5,20,21].

Table 1. Protein bar formulations.

Ingredients	Control Protein Bar (g/100 g)	Fortified Protein Bar * (g/100 g)
Whey protein concentrate	38.66	37.06
Brown rice flour	19.33	18.53
Spirulina powder	0	2
Phycocyanin powder	0	0.4
Glycerin	16.01	16.01
Sunflower oil	9.80	9.80
water	16.20	16.20

* Fortified protein bar contains 2% spirulina powder and 0.4% phycocyanin powder.

2.2.2. Moisture content

Moisture content was determined using the oven-drying method. Approximately 4–5 g of ground sample was dried in a hot-air oven at 105 °C for 5 h, cooled in a desiccator to room temperature, and weighed [22]. Moisture percentage was calculated using Equation (1):

$$\text{Moisture content (\%)} = \frac{W_S-(W_2-W_1)}{W_S} \times 100 \quad (1)$$

where W_S is the sample weight (g), W_1 is the empty dish weight (g), and W_2 is the weight of the dish and dried sample (g).

2.2.3. Water activity

Water activity (aw) was measured using a

LabTouch-aw device (Novasina, Switzerland) at 25 °C.

2.2.4. Titratable acidity

For titratable acidity, 1 g of sample was dispersed in 200 mL of distilled water and left at room temperature for 1 h to achieve equilibrium. Then, 0.5 mL of 1% phenolphthalein solution indicator was added, and titration was performed with 0.1 N NaOH until a faint pink color persisted for at least 30 s. The consumed NaOH volume was recorded, adjusted to the equivalent of 5 g sample in 50 mL water, and expressed as lactic acid percentage using Equation (2) [23]:

$$\text{Titratable acidity (\% lactic acid)} = \frac{\text{V} \times \text{N} \times 0.09 \times 100}{m} \quad (2)$$

where V represents the volume of NaOH consumed (mL), N is the normality of NaOH, 0.09 is the equivalent factor of lactic acid, and m denotes the sample weight (g).

2.2.5. Peroxide value

Peroxide value was determined by extracting 4 g of homogenized sample with 10 mL chloroform and 15 mL glacial acetic acid, left for 30 min in the dark at room temperature. The filtrate was treated with 1 mL saturated KI solution and kept in the dark for 5 min, followed by the addition of 1 mL distilled water and 0.5 mL of 1% starch solution indicator. Titration with 0.01 M sodium thiosulfate was performed until the solution became colorless. The peroxide value (meq O_2/kg) was calculated using Equation (3) [24]:

$$PV = \frac{(V_1 - V_0)T \times 10^3}{M} \quad (3)$$

In this equation, V_1 represents the volume of thiosulfate used for the sample (mL), V_0 is the blank value (mL), T denotes the molarity of thiosulfate, and M is the sample mass (g).

2.2.6. Color measurement

Color attributes were evaluated using digital image analysis. Three regions per sample were photographed with a Samsung S8 camera (12 MP) at a fixed distance of 9.5 cm under constant ceiling light, using a neutral background and avoiding shadows. Images were saved in JPEG format and analyzed using ImageJ software (version 1.52v). Pixel regions of the samples were extracted, converted from RGB to CIELab space, and L*, a*, b* values were obtained [25, 26]. Total color difference (ΔE) was calculated by Equation (4):

$$\Delta\text{E} = \sqrt{(L_0 - L)^2 + (a_0 - a)^2 + (b_0 - b)^2} \quad (4)$$

where L, a, b represent sample color parameters and L_0, a_0, b_0 were taken as baseline values (zero).

2.2.7. Kinetic analysis during storage

Kinetic modeling, data analysis, and plotting of physicochemical and color changes in control and fortified protein bars were performed using MATLAB software (version 24). Fourteen different mathematical models were tested to fit the data. Model performance was evaluated using statistical indices including the coefficient of determination (R^2), chi-square (χ^2), mean bias error (MBE), and root mean square error (RMSE), calculated by Equations (5) to (8):

$$HR = \frac{\text{H}_\infty - \text{H}_\text{t}}{\text{H}_\infty - \text{H}_0} \quad (5)$$

$$\chi 2 = \frac{\sum_{i=1}^{N}(HR_{exp,i} - HR_{pre,i})^2}{N - n} \quad (6)$$

$$MBE = \frac{1}{N}\sum_{i=1}^{N}(HR_{pre,i} - HR_{exp,i}) \quad (7)$$

$$RMSE = \left[\frac{1}{N}\sum_{i=1}^{N}\left(HR_{pre,i} - HR_{exp,i}\right)^2\right]^{\frac{1}{2}} \quad (8)$$

Where, H_0 represents the physicochemical changes of the protein bar at time zero, H_∞ indicates the physicochemical changes occurring over storage time, and H_t denotes the physicochemical changes of the protein bar at time t. $HR_{exp,i}$ refers to the experimental values obtained from the analysis of physicochemical properties, while $HR_{pre,i}$ corresponds to the predicted values of these properties. N is the number of observations, and n is the number of constants [27]. Statistical differences between kinetic parameters of control and fortified samples were determined using an independent samples t-test at a significance level of $p < 0.05$.

3. Results and discussion

3.1. Kinetic analysis during storage

Protein bars, as protein-rich food products, are subject to physical and chemical changes during storage. Monitoring variations in moisture, water activity, titratable acidity, peroxide value, and color difference (ΔE) in both control and fortified samples is crucial for assessing product quality and shelf life. To model these changes over storage time, 14 empirical regression models—including linear, quadratic, Weibull, Gompertz, Harris, Rational, Newton, Page, Logarithmic, Exponential, Logistic, Two Term, Diffusion, and Fourier models—were evaluated. The statistical performance of these models, including goodness-of-fit indices and estimated parameters, along with comparative analyses between the control and fortified samples, are summarized in Tables (2) to (11). Graphical representations of the best-fitting models for each parameter are presented in Fig. 1. to 5. Generally, models with higher R^2 values and lower MBE, RMSE, and χ^2 values were considered more accurate for describing the kinetic behavior of the samples [27].

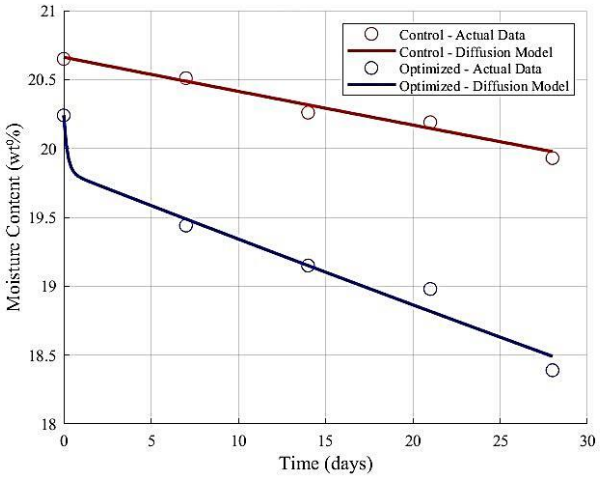

Fig. 1. Diffusion model fitting graph for moisture changes in control and fortified protein bars during storage time.

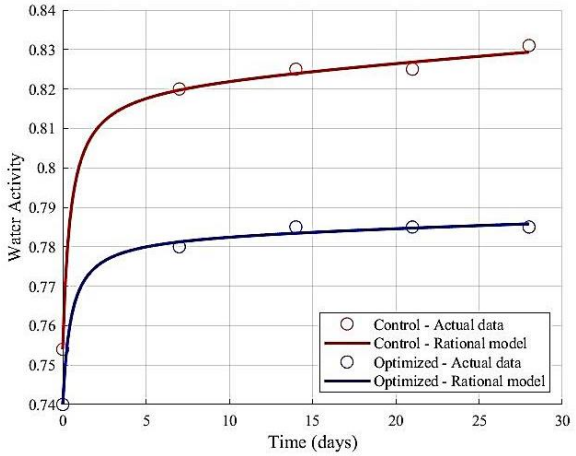

Fig. 2. Rational model fitting graph for water activity changes in control and fortified protein bars during storage time.

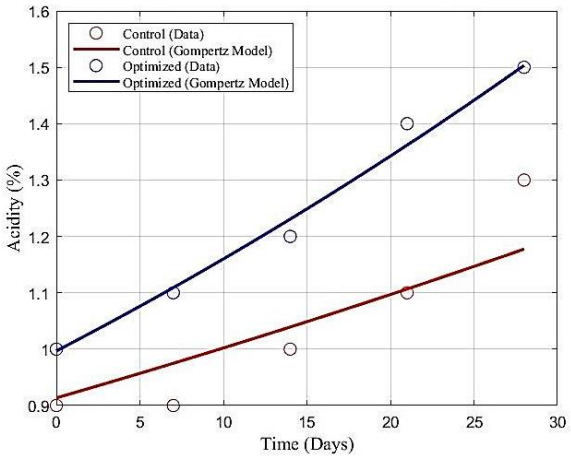

Fig. 3. Gompertz model fitting graph for acidity changes in control and fortified protein bars during storage time.

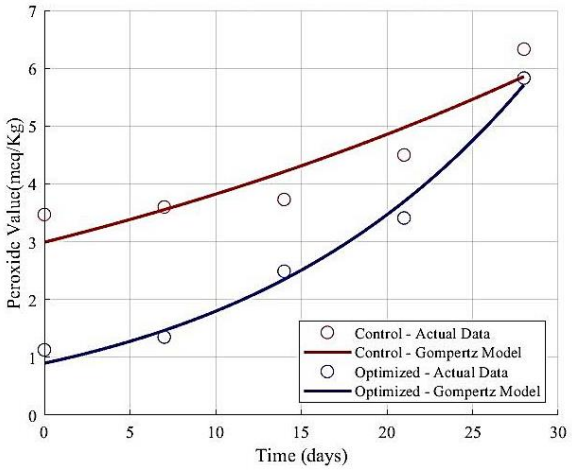

Fig. 4. Gompertz model fitting graph for peroxide changes in control and fortified protein bars during storage time.

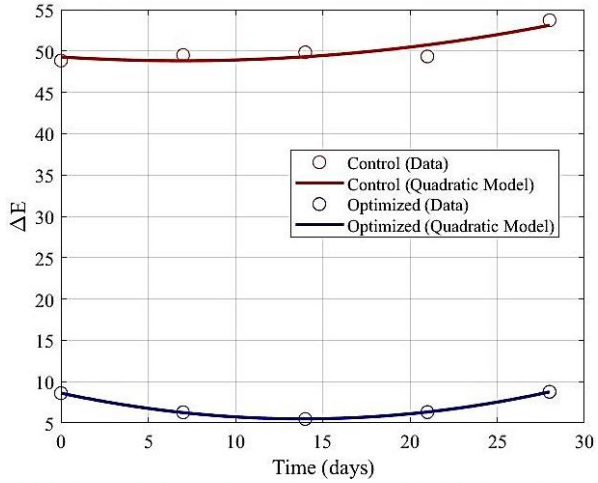

Fig. 5. Quadratic model fitting graph for ΔE changes in control and fortified protein bars during storage time.

3.2. Moisture content

Moisture content decreased progressively over the 28-day storage period in both control and fortified protein bars. The reduction was more pronounced in the fortified bars, likely due to the influence of spirulina and phycocyanin on the product structure. These bioactive components may have altered the microstructure and increased porosity, thereby facilitating moisture loss during storage [28].

Kinetic modeling was performed to further analyze these differences. Model selection was based on fitting accuracy, using R^2, RMSE, χ^2, and MBE as criteria (Table 2). Among the tested models, the Diffusion model provided the best fit, with high R^2 values (0.977 for the control and 0.979 for the fortified sample) and low RMSE and χ^2 values. Notably, the fortified sample showed the lowest χ^2 (2.07×10^{-3}), indicating superior fitting accuracy. The low RMSE values in both cases also confirmed the model's predictive reliability. Based on these criteria, the Diffusion model was selected as the most appropriate for describing the moisture kinetics of both protein bar formulations. The general form of the Diffusion model was expressed as:

$$C_t = a \exp(-bt) + (1-c) \exp(-cdt) \quad (9)$$

Table 2. Results of the statistical analysis obtaind from modelling the changes in Moisture in control and fortified protein bar samples.

Model No.	Name	Model equation	Constants		R^2		MBE		RMSE		χ^2	
			Control	Fortified	Control	Fortified	Control	Fortified	Control	Fortified	Control	Fortified
1	Linear	$C_t = a + bt$	a= 20.66 b= -0.0251	a= 20.072 b= -0.0594	0.978	0.941	2.132×10^{-15}	1.421×10^{-15}	0.0377	0.1467	3.52×10^{-4}	5.51×10^{-3}
2	Quadratic	$C_t = a + bt + Ct^2$	a= 20.651 b= -0.0227 c= -0.0001	a= 20.1491 b= -0.0815 c= 0.0008	0.978	0.953	7.105×10^{-16}	2.132×10^{-15}	0.0371	0.13177	3.39×10^{-4}	4.53×10^{-3}
3	Weibull	$C_t = b/c\,(t-a)^{(b-1)}\,e^{-((t-a)/c)b}$	a= 0 b= 0.7740 c= 6.82	a= 0 b= 0.7748 c= 2.34	-515.8	-782.42	-16.163	-15.177	18.071	16.971	1.1633×10^{5}	1.0133×10^{5}

Model No.	Name	Model equation	Constants		R^2		MBE		RMSE		χ^2	
			Control	Fortified	Control	Fortified	Control	Fortified	Control	Fortified	Control	Fortified
4	Gompertz	$C_t = a.\exp(-\exp(-b(c-x)))$	a= 21.564 b= 0.0217 c= 82.755	a= 25.7973 b= 0.0101 c= 130.2197	0.975	0.932	-3.23×10^{-4}	2.43×10^{-4}	0.0396	0.15783	3.86×10^{-4}	6.34×10^{-3}
5	Harris	$C_t = 1 / (a + bt^c)$	a= 0.0484 b= 0 c= 1.0827	a= 0.0494 b= 0.0005 c= 0.6875	0.978	0.969	1.851×10^{-7}	1.2673×10^{-5}	0.0373	0.10645	3.44×10^{-4}	3.01×10^{-3}
6	Rational	$C_t = (a + bt) / (1+ct+dt^2)$	a= 10.780 b= 0 c= -0.0138 d= -0.0002	a= 20.24 b= 6323.804 c= 318.678 d= 0.8262	-709.85	0.978	-5.224	1.9101×10^{-5}	6.712	0.0902	18.79	2.17×10^{-3}
7	Newton	$C_t = \exp(-at)$	a= 0	a= 0	-5882.3	-904.95	-19.308	-18.24	19.31	18.25	1864.3	1665.3
8	Page	$C_t = \exp(-at^b)$	a= 0 b= 1.5122	a= 0 b= 1.5124	-5882.3	-904.95	-19.308	-18.24	19.31	18.25	1864.3	1665.3
9	Logarithmic	$C_t = a\exp(-bt) + c$	a= 16.904 b= 0.0015 c= 3.7574	a= 2.6486 b= 0.0356 c= 17.5284	0.977	0.957	3.4016×10^{-6}	1.3685×10^{-6}	0.03806	0.12641	3.59×10^{-4}	4.20×10^{-3}
10	Exponential	$C_t = a(b-\exp(-ct))$	a= 0.05 b= 406.61 c= 3.3203	a= 20.0832 b= -0.0031	-0.114	0.944	-0.0017	-2.316×10^{-5}	0.26573	0.14351	0.0174	5.28×10^{-3}
11	Logistic	$C_t = a / (1 + b\exp(-ct))$	a= 20.308 b= 0 c= 6.0734	a= 19.24 b= 0 c= 5.4321	-1.4952×10^{-12}	-5.91×10^{-13}	-1.109×10^{-12}	-2.37×10^{-12}	0.25175	0.60633	0.015604	0.095541
12	Two-term	$C_t = a\exp(-bt)+c\exp(-dt)$	a= 10.337 b= 0.0012 c= 10.325 d= 0.0012	a= 0.0004 b= -0.003 c= 20.0828 d= 0.0031	0.977	0.944	5.2633×10^{-7}	-2.317×10^{-5}	0.038	0.14351	3.57×10^{-4}	5.28×10^{-3}
13	Diffusion	$C_t = a\exp(-bt) + (1-c)\exp(-cdt)$	a= 19.726 b= 0.0012 c= 0.0644 d= 0.0199	a= 19.8319 b= 0.0025 c= 0.5919 d= 8.1757	0.977	0.979	2.6396×10^{-6}	9.4047×10^{-6}	0.038	0.08814	3.57×10^{-4}	2.07×10^{-3}
14	Fourier	$C_t = a+b\cos(ct) + d\sin(ct)$	a= -734589.37 b= 734610.03 c= 0 d= -1470.65	a= 1640218.48 b= -1640198.33 c= 0 d= 2629.62	0.978	0.953	1.531×10^{-11}	-5.01×10^{-10}	0.03705	0.13177	3.39×10^{-4}	4.53×10^{-3}

As shown in Table 3, the parameter a (initial C_t value) was similar in both samples (19.7 and 19.8), with no significant difference at the 95% confidence level. However, b (rate of initial decline) was nearly double in the fortified bar (0.0025) compared to the control (0.0012), suggesting a faster initial decrease. The parameter c, associated with long-term changes, was substantially higher in the fortified sample (0.5919) than in the control (0.0644), indicating a stronger influence on long-term moisture decline. Likewise, d was markedly higher in the fortified bar (8.1757) compared to the control (0.0199), reflecting more rapid progression toward equilibrium. Overall, the higher values of b, c, and d in the fortified protein bars indicate accelerated kinetic behavior and faster attainment of equilibrium compared to the control. This difference can be attributed to the presence of spirulina and phycocyanin, which influenced product structure and interactions within the protein matrix. Phycocyanin, as a protein-pigment containing charged functional groups, may interact with other proteins through hydrogen bonding and electrostatic forces, affecting structural stability. Its antioxidant activity may also interfere with secondary interactions between proteins and lipid oxidation products, thereby altering reaction pathways. Such interactions may accelerate certain degradation processes or trigger new ones, leading to faster kinetics [29,30]. Additionally, spirulina, rich in proteins, polysaccharides, and bioactive pigments, can affect the protein matrix and overall stability of the product. Its bioactive compounds may increase intermolecular interactions and alter moisture behavior, thereby enhancing the rate of change during storage. These compounds may also influence water permeability and moisture distribution within the product, leading to faster kinetics. Chemical interactions induced by spirulina and phycocyanin thus likely contributed to reduced stability and increased rates of physicochemical reactions [10,31]. The observed differences in kinetic behavior between the control and fortified protein bars can therefore be explained by the combined effects of antioxidant activity, protein interactions, and modified moisture dynamics associated with spirulina and phycocyanin, as reflected in the selected Diffusion model.

Table 3. Statistical comparison of the diffusion model constants for moisture.

Constant	Control	Fortified	p-value
a	19.7257(*a)	19.8319(a)	0.85
b	0.0012(b)	0.0025(a)	0.01
c	0.0644(b)	0.5919(a)	0.001
d	0.0199(b)	8.1757(a)	0.0001

*Values with different letters in each row indicates a significant difference at the 0.05 level, while values with the same letters are not significantly different.

Consistent with our findings, Al-Baarri *et al.* [32] also reported a decreasing trend in moisture content in corn-based snack bars during 0–35 days of storage. This reduction was attributed to water vapor migration from the product to the surrounding environment, driven by the moisture gradient between the product and its storage atmosphere.

3.3. Water activity

Water activity (aw) showed an increasing trend during storage in both control and fortified protein bars, although the extent of increase was lower in the fortified samples. This difference may be attributed to the water-binding and emulsifying properties of spirulina and phycocyanin. By absorbing and binding water molecules, these compounds reduce the proportion of free water in the system, thereby limiting its availability. A reduction in water activity is generally considered advantageous for food stability, as it decreases the risk of microbial spoilage and prolongs shelf life [3,33]. Similar behavior, where water activity increased despite decreasing moisture content, was reported in muffins formulated with water chestnut and barley flour during 35 days of storage [34].

Table 4. Results of the statistical analysis obtaind from modelling the changes in water activity in control and fortified protein bar samples.

Model No.	Name	Model equation	Constants		R^2		MBE		RMSE		χ^2	
			Control	Fortified	Control	Fortified	Control	Fortified	Control	Fortified	Control	Fortified
1	Linear	$C_t = a + bt$	a= 0.0023 b= 0.7792	a= 0.0014 b= 0.756	0.613	0.582	0	0	0.017854	0.01138	0.002006	8.45×10^{-4}
2	Quadratic	$C_t = a + bt + Ct^2$	a= -0.0002 b= 0.0074 c= 0.7613	a= -0.0001 b= 0.0048 c= 0.7439	0.884	0.915	1.1102×10^{-16}	6.6613×10^{-17}	0.009776	0.005127	5.91×10^{-4}	1.70×10^{-4}
3	Weibull	$C_t = b/c\ (t-a)^{(b-1)}\ e^{-((t-a)/c)b}$	a= 0 b= 0.9087 c= 9.0179	a= 0 b= 0.9091 c= 9.101	-625.15	-1496.4	-0.64312	-0.6099	0.71847	0.68131	168.74	150.56
4	Gompertz	$C_t = a.exp(-exp(-b(c-x)))$	a= 0.8453 b= -0.0775 c= -24.886	a= 0.7953 b= -0.0804 c= -27.5931	0.822	0.822	-7.895×10^{-5}	-8.078×10^{-5}	0.01213	0.007427	9.28×10^{-4}	3.60×10^{-4}
5	Harris	$C_t = 1 / (a + bt^c)$	a= 1.233 b= 0 c= 0	a= 1.2903 b= 0 c= 0	-8.1031×10^{-10}	-1.4127×10^{-9}	-6.850×10^{-8}	-5.7345×10^{-7}	0.028712	0.017607	0.0050826	0.002
6	Rational	$C_t = (a + bt) / (1+ct+dt^2)$	a= 0.754 b= 1.7647 c= 2.147 d= -0.0008	a= 0.74 b= 1.5785 c= 2.0151 d= -0.0003	0.998	0.997	8.9828×10^{-8}	1.5544×10^{-7}	0.001165	9.67×10^{-4}	8.1984×10^{-6}	5.972×10^{-6}
7	Newton	$C_t = exp(-at)$	a= 0.0094	a= 0.0121	-18.561	-60.735	0.069701	0.075302	0.12699	0.13834	0.083087	0.10017
8	Page	$C_t = exp(-at^b)$	a= 0.2095 b= 0	a= -0.2549 b= 0	-2.3618×10^{-10}	-7.77×10^{-8}	1.0694×10^{-8}	1.5298×10^{-7}	0.028712	0.017607	0.0050826	0.002
9	Logarithmic	$C_t = a\ exp(-bt) + c$	a= 0.8604 b= 0 c= -0.0494	a= 0.0003 b= 0 c= 0.7746	-4.7414×10^{-9}	-1.6156×10^{-5}	2.0349×10^{-7}	-7.029×10^{-5}	0.028712	0.017607	0.0050826	0.002
10	Exponential	$C_t = a\ (b-exp(-ct))$	a= 0.0734 b= 11.270 c= 0.3193	a= 0.0452 b= 17.3732 c= 0.3114	0.995	0.9999	-1.713×10^{-7}	5.1606×10^{-8}	0.002049	2.03×10^{-4}	2.5381×10^{-5}	2.621×10^{-7}
11	Logistic	$C_t = a / (1 + b\ exp(-ct))$	a= 0.8274 b= 0.0973 c= 0.3323	a= 0.7852 b= 0.0611 c= 0.319	0.995	0.9999	-2.1602×10^{-7}	-2.553×10^{-8}	0.002061	1.94×10^{-4}	2.5672×10^{-5}	2.391×10^{-7}
12	Two-term	$C_t = a\ exp(-bt)+c\ exp(-dt)$	a= 0.4055 b= 0 c= 0.4055 d= 0	a= 0.3875 b= 0 c= 0.3875 d= 0	-4.5755×10^{-11}	-5.8416×10^{-8}	-7.912×10^{-10}	-3.049×10^{-8}	0.028712	0.017607	0.005083	0.002
13	Diffusion	$C_t = a\ exp(-bt) + (1-c)\ exp(-cdt)$	a= 0.0015 b= 0 c= 0.1905 d= 0	a= 0.0019 b= 0 c= 0.2269 d= 0	-8.1028×10^{-10}	-8.9605×10^{-10}	8.1636×10^{-7}	5.2601×10^{-7}	0.028712	0.017607	0.005083	0.002
14	Fourier	$C_t = a+b\ cos(ct) + d\ sin(ct)$	a= -65667.349 b= 65668.11 c= -0.0001 d= -98.9786	a= -34983.0612 b= 34983.805 c= 0.0001 d= 57.3464	0.884	0.915	2.1775×10^{-11}	4.4692×10^{-12}	0.009776	0.005127	5.91×10^{-4}	0.001698

Among the evaluated models, the Rational model was identified as the best fit for describing the kinetic changes in water activity (Table 4). The general form of this model is:

$$C_t = (a + bt) / (1+ct+dt^2) \quad (10)$$

where C_t is the water activity at time t, and a,b,c, and d are regression coefficients estimated from experimental data. As summarized in Table 5, parameter a represents the initial water activity (y-intercept), which did not differ significantly between control and fortified samples. Parameter b reflects the initial rate of increase; its higher value in the control bar indicates greater early-stage changes. Parameter c moderates the growth rate; higher values, as seen in the control, suggest a more controlled progression of aw over time. Finally, parameter d accounts for nonlinear contributions, with higher positive values in the control pointing to a gradual slowdown of aw increase at later stages.

Previous studies have also modeled aw kinetics in various food systems. For example, Srisuk and Jirasatid [35] applied a zero-order kinetic model to describe water activity changes in pumpkin–fingerroot drink powders stored at 4, 32, and 45 °C for 70 days, while Tireki *et al.* [36] successfully used a Weibull model to explain aw changes in candies stored for 12 weeks at 10–30 °C.

Table 5. Statistical comparison of the rational model constants for water activity.

Constant	Control	Fortified	p-value
a	0.754 (*a)	0.74(a)	0.185
b	1.765 (a)	1.579 (b)	0.002
c	2.147 (a)	2.015 (b)	0.006
d	-0.0008 (b)	-0.0003(a)	0.021

*Values with different letters in each row indicates a significant difference at the 0.05 level, while values with the same letters are not significantly different.

3.4. Titratable acidity

Titratable acidity increased in both protein bar formulations during 28 days of storage, with a greater rise observed in the fortified samples. Spirulina powder, which contains approximately 14% lactic acid, may have directly contributed to this higher acidity level. Among the tested kinetic models, the Gompertz model provided the best fit for both formulations (Table 6), expressed as:

$$C_t = a.\exp[-\exp(-b(c-x))] \quad (11)$$

Table 6. Results of the statistical analysis obtaind from modelling the changes in acidity in control and fortified protein bar samples.

Model No.	Name	Model equation	Constants		R^2		MBE		RMSE		χ^2	
			Control	Fortified	Control	Fortified	Control	Fortified	Control	Fortified	Control	Fortified
1	Linear	$C_t = a + bt$	a= 0.0143 b= 0.84	a= 0.0186 b= 0.98	0.893	0.983	8.882×10^{-17}	6.661×10^{-17}	0.04899	0.024495	0.011833	0.0024455
2	Quadratic	$C_t = a + bt + Ct^2$	a= 0.0006 b= -0.002 c= 0.8971	a= 0.0001 b= 0.0145 c= 0.9943	0.995	0.987	8.882×10^{-17}	1.332×10^{-16}	0.01069	0.021381	5.75×10^{-4}	0.0017268
3	Weibull	$C_t = b/c\ (t-a)^{(b-1)}\ e^{-((t-a)/c)b}$	a= 0 b= 0.8982 c= 9.364	a= 0 b= 0/8940 c= 9.2175	-39.506	-37.66	-0.84311	-1.0232	0.95254	1.1532	324.09	466.18
4	Gompertz	$C_t = a.\exp(-\exp(-b(c-x)))$	a= 3.6298 b= -0.0403 c= 43.833	a= 1.7321 b= -0.0824 c= 15.5455	0.994	0.992	9.9826×10^{-7}	-7.708×10^{-v}	0.01205	0.01656	7.60×10^{-4}	0.001107
5	Harris	$C_t = 1 / (a + bt^c)$	a= 0.9615 b= 0 c= 0	a= 0.8065 b= 0 c= 0	-1.5204×10^{-10}	-6.0443×10^{-12}	1.8391×10^{-6}	4.5311×10^{-7}	0.14967	0.18547	0.10769	0.13871
6	Rational	$C_t = (a + bt) / (1+ct+dt^2)$	a= 0.9 b= 13.129 c= 16.224 d= -0.2162	a= 0.9999 b= 12.829 c= 12.6058 d= -0.1494	0.994	0.982	-1.23×10^{-4}	1.55×10^{-4}	0.011969	0.024713	6.42×10^{-4}	0.0022615
7	Newton	$C_t = \exp(-at)$	a= 0	a= 0	-0.071	-1.6744	-0.04	-0.24	0.15492	0.30332	0.12	0.46
8	Page	$C_t = \exp(-at^b)$	a= 0 b= 0	a= 0 b= 0	-0.071	-1.6744	-0.04	-0.24	0.15492	0.30332	0.12	0.46
9	Logarithmic	$C_t = a\exp(-bt) + c$	a= 0.0001 b= 0.0001 c= 1.0398	a= 0.0094 b= 0 c= 1.2306	-1.1089×10^{-6}	-3.193×10^{-11}	-4.093×10^{-5}	-2.037×10^{-8}	0.14967	0.18547	0.1077	0.13871
10	Exponential	$C_t = a\ (b-\exp(-ct))$	a= 21.664 b= 1.0386 c= 0.0007	a= 9.027 b= 1.1079 c= 0.0021	0.891	0.981	$8.82\text{-}\times10^{-4}$	-0.001475	0.049403	0.025464	0.012135	0.0027069
11	Logistic	$C_t = a / (1 + b\ \exp(-ct))$	a= 145.77 b= 171.88 c= 0.0144	a= 6.3125 b= 5.3769 c= 0.0188	0.925	0.986	-3.23×10^{-4}	-4.293×10^{-5}	0.04096	0.021648	0.008484	0.0018109
12	Two-term	$C_t = a\exp(-bt)+c\exp(-dt)$	a= 0.52 b= 0 c= 0.52 d= 0	a= 0.62 b= 0 c= 0.62 d= 0	-6.9238×10^{-10}	-2.9134×10^{-12}	-5.543×10^{-8}	6.156×10^{-12}	0.14967	0.18547	0.10769	0.13871
13	Diffusion	$C_t = a\exp(-bt) + (1-c)\exp(-cdt)$	a= 0.0582 b= 0 c= 0.0182 d= 0	a= 0.2587 b= 0 c= 0.0187 d= 0	-5.2833×10^{-10}	-1.1652×10^{-10}	-2.541×10^{-7}	-5.969×10^{-8}	0.14967	0.18547	0.10769	0.13871
14	Fourier	$C_t = a+b\cos(ct) + d\sin(ct)$	a= 83101145.7 b= -83101144.8 c= 0 d= -544.7832	a= 1.2728 b= -0.2679 c= 0.845 d= 0.0576	0.995	0.993	-1.526×10^{-8}	-1.33×10^{-16}	0.01069	0.015747	5.75×10^{-4}	0.0010205

In this equation, a represents the maximum acidity attainable by the product, b describes the rate of change, and c indicates the time at which the steepest increase occurs. As shown in Table 7, the maximum acidity (a) was higher in the control (3.6298) compared to the fortified bar (1.7321), suggesting that overall acidity remained lower in the fortified formulation. Parameter b showed no significant difference between the two samples. Interestingly, parameter c was markedly lower in the fortified bar (15.5455 vs. 43.8325 in the control), indicating that the most intense changes occurred earlier. This accelerated acidification may be linked to the presence of spirulina, which provided both lactic acid and microbial substrates that facilitated faster increases in acidity.

Table 7. Statistical comparison of the gompertz model constants for acidity.

Constant	Control	Fortified	p-value
a	3.6298(*a)	1.7321(b)	0.002
b	-0.0403(a)	-0.0824(a)	0.087
c	43.8325(a)	15.5455(b)	0.001

*Values with different letters in each row indicates a significant difference at the 0.05 level, while values with the same letters are not significantly different.

Comparable findings were reported by Yang *et al.* [37], who applied the Arrhenius model to predict the shelf life of vacuum-packed noodles at 25 °C, where acidity was also a critical determinant of product stability.

3.5. Peroxide value

Peroxide value, an indicator of primary lipid oxidation, increased in both control and fortified protein bars during storage. However, the extent of increase was lower in the fortified samples, suggesting that antioxidant compounds in spirulina and phycocyanin slowed the oxidative process.

Kinetic analysis revealed that the Gompertz model best described the peroxide value changes for both formulations (Table 8), supported by high R^2 values (0.999 for control and 0.985 for fortified protein bars) and low RMSE and χ^2 values. The model equation is:

$$C_t=a.\exp[-\exp(-b(c-x))] \quad (12)$$

Table 8. Results of the statistical analysis obtaind from modelling the changes in peroxide in control and fortified protein bar samples.

Model No.	Name	Model equation	Constants		R^2		MBE		RMSE		χ^2	
			Control	Fortified	Control	Fortified	Control	Fortified	Control	Fortified	Control	Fortified
1	Linear	$C_t = a + bt$	a= 3.002 b= 0.0946	a= 0.55 b= 0.1637	0.774	0.904	8.882×10^{-17}	1.044×10^{-15}	0.50574	0.52887	0.28577	0.90395
2	Quadratic	$C_t = a + bt + Ct^2$	a= 3.5791 b= -0.0703 c= 0.0059	a= 1.1471 b= -0.0069 c= 0.0061	0.980	0.990	4.441×10^{-16}	4.441×10^{-17}	0.15037	0.17349	0.02853	0.0515
3	Weibull	$C_t = b/c\ (t-a)^{(b-1)}\ e^{-((t-a)/c)b}$	a= 0 b= 0.9972 c= 0.3068	a= 0 b= 0.8809 c= 12.18	-14.401	-2.6614	-3.632	-2.6005	4.1759	3.2621	2.276×10^{40}	4341.6
4	Gompertz	$C_t = a.\exp(-\exp(-b(c-x)))$	a= 142.80 b= -0.034 c= 67/9698	a= 24277.46 b= -0.0074 c= 317/1005	0.999	0.985	-6.896×10^{-7}	0.04856	0.03164	0.21242	1.40×10^{-3}	0.08226
5	Harris	$C_t = 1 / (a + bt^c)$	a= 0.231 b= 0.0002 c= 0	a= 0.3516 b= 0.0003 c= 0	-1.5365×10^{-13}	-6.0757×10^{-11}	-7.09×10^{-10}	-1.376×10^{-7}	1.0641	1.7048	1.3087	5.1132
6	Rational	$C_t = (a + bt) / (1+ct+dt^2)$	a= 3.5074 b= 0 c= 0.0055 d= -0.0008	a= 1.0577 b= 0.0363 c= -0.0221 d= 0	0.998	0.994	-4.68×10^{-4}	2.7156×10^{-6}	0.05204	0.13709	3.80×10^{-3}	0.05145
7	Newton	$C_t = \exp(-at)$	a= 0	a= 0	-9.7701	-1.1674	-3.326	-1.842	3.4921	2.5098	60.973	31.497
8	Page	$C_t = \exp(-at^b)$	a= 0 b= 2.5	a= 0 b= 0	-9.7701	-1.1674	-3.326	-1.842	3.4921	2.5098	60.973	31.497
9	Logarithmic	$C_t = a \exp(-bt) + c$	a= 0.1774 b= 0 c= 4.1486	a= 0 b= 0 c= 2.842	-6.4783×10^{-8}	-6.8002×10^{-10}	-2.999×10^{-8}	-4.445×10^{-5}	1.0641	1.7048	1.3087	5.1133
10	Exponential	$C_t = a\ (b-\exp(-ct))$	a= 380.2421 b= 1.0079 c= 0.0003	a= 1374.4766 b= 1.0004 c= 0.0001	0.773	0.904	-5.38×10^{-3}	-1.58×10^{-3}	0.507	0.52963	0.289	0.91402
11	Logistic	$C_t = a / (1 + b \exp(-ct))$	a= 28048.953 b= 9356.501 c= 0.024	a= 15703.6982 b= 16658.8757 c= 0.0645	0.847	0.990	-9.40×10^{-3}	-0.01375	0.41648	0.17133	0.20601	0.07805
12	Two-term	$C_t = a \exp(-bt)+c \exp(-dt)$	a= 2.1624 b= 0 c= 2.1624 d= 0	a= 1.421 b= 0 c= 1.421 d= 0	-1.1453×10^{-6}	-9.6079×10^{-12}	-1.14×10^{-3}	-5.088×10^{-6}	1.0641	1.7048	1.309	5.1132
13	Diffusion	$C_t = a \exp(-bt) + (1-c) \exp(-cdt)$	a= 3.3498 b= 0 c= 0.0238 d= 0	a= 1.8654 b= 0 c= 0.0234 d= 0	-1.2261×10^{-12}	-4.6296×10^{-13}	-4.749×10^{-9}	1.9326×10^{-8}	1.0641	1.7048	1.3087	5.1132
14	Fourier	$C_t = a+b \cos(ct) + d \sin(ct)$	a=1.09×10^6 b= -1.09×10^6 c= -0.0001 d= 675.604	a= 3.78×10^7 b= -3.78×10^7 c= 0 d= 384.362	0.980	0.990	-1.62×10^{-10}	-9.934×10^{-9}	0.15037	0.17349	0.02853	0.0515

Here, a denotes the maximum peroxide value, b the rate of increase, and c the time required to approach the final oxidation phase. As reported in Table 9, the maximum peroxide value (a) was considerably higher in the fortified protein bars (24277.458) than in the control (142.803), indicating greater overall lipid oxidation potential. However, the rate parameter (b) was lower in the fortified samples, implying a slower accumulation of peroxides. Additionally, the higher c value in the fortified bar (317.1005 vs. 67.9698 in control) suggests that the transition to the final oxidation phase was delayed.

Table 9. Statistical comparison of the gompertz model constants for peroxide.

Constant	Control	Fortified	p-value
a	142.803(*b)	24277.458(a)	0.0001
b	-0.034(a)	-0.0074(b)	0.02
c	67.9698(b)	317.1005(a)	0.0001

*Values with different letters in each row indicates a significant difference at the 0.05 level, while values with the same letters are not significantly different.

This dual behavior, characterized by higher ultimate peroxide values but slower progression, can be

explained by the presence of phycocyanin and other bioactive compounds in spirulina. These compounds may simultaneously provide antioxidant protection and alter the product matrix in ways that influence oxidation dynamics. Similar approaches have been used in other studies: Manzocco *et al.* [38] applied a zero-order model to predict cracker shelf life based on peroxide formation, while another study used a first-order kinetic model to describe peroxide changes in safflower oil fortified with phycocyanin and BHT [39].

3.6. Color difference (ΔE)

The color difference (ΔE) of control protein bars increased steadily throughout 28 days of storage. In contrast, fortified samples showed a decrease in ΔE until day 14, followed by an increase until day 28. However, the total increase in ΔE remained lower in fortified samples than in the controls.The initial decline suggests stabilization of the color profile, while the later increase may reflect secondary reactions or environmental effects influencing pigments. By day 28, ΔE values appeared to stabilize, indicating the attainment of final color equilibrium. Among the tested models, the Quadratic provided the best fit for both formulations (Table 10), expressed as:

$$C_t = a + bt + Ct^2 \quad (13)$$

Table 10. Results of the statistical analysis obtaind from modelling the changes in ΔE in control and fortified protein bar samples.

Model No.	Name	Model equation	Constants		R^2		MBE		RMSE		χ^2	
			Control	Fortified	Control	Fortified	Control	Fortified	Control	Fortified	Control	Fortified
1	Linear	$C_t = a + bt$	a= 0.137 b= 48.33	a= 0.0053 b= 7.756	0.590	0.002	8.527×10^{-15}	3.553×10^{-16}	1.13	1.3352	0.12421	1.2568
2	Quadratic	$C_t = a + bt + Ct^2$	a= 0.0096 b= -0.1328 c= 49.274	a= 0.0163 b= -0.4506 c= 8.6137	0.791	0.9998	2.842×10^{-15}	1.776×10^{-16}	0.80789	0.018578	0.06464	2.70×10^{-4}
3	Weibull	$C_t = b/c\ (t-a)^{(b-1)}\ e^{-((t-a)/c)b}$	a= 0 b= 0.7386 c= 4.59	a= 0 b= 0.9992 c= 0.1182	-656.66	-19.885	-40.467	-5.372	45.27	6.1066	$7.868\times10^{+5}$	$3.42\times10^{+103}$
4	Gompertz	$C_t = a.\exp(-\exp(-b(c-x)))$	a= 4406.4264 b= -0.0042 c= 475.5954	a= 8.7701 b= -2.0851 c= 23.0887	0.655	0.394	0.014238	1.599×10^{-15}	1.037	1.04	0.10449	0.81047
5	Harris	$C_t = 1 / (a + bt^c)$	a= 0.0199 b= 0 c= 0	a= 0 b= 0.1449 c= 0.0093	0	0.296	1.244×10^{-10}	-3.38×10^{-4}	1.7653	1.1214	0.31008	0.9377
6	Rational	$C_t = (a + bt) / (1+ct+dt^2)$	a= 42.757 b= 0 c= -0.0013 d= -0.0002	a= 8.6146 b= 0 c= 0.0752 d= -0.0027	-4.743	0.994	-3.0532	0.0011062	4.2306	0.10415	2.0453	0.0092414
7	Newton	$C_t = \exp(-at)$	a= 0	a= 0	-778.3	-20.786	-49.248	-6.092	49.28	6.2368	12142	194.49
8	Page	$C_t = \exp(-at^b)$	a= 0 b= 0.6237	a= 0 b= 0.6238	-778.3	-20.786	-49.248	-6.092	49.28	6.2368	12142	194.49
9	Logarithmic	$C_t = a \exp(-bt) + c$	a= 0.3516 b= 0 c= 49.896	a= 1.885 b= 3.6022 c= 6.715	-7.8826×10^{-14}	0.318	-9.147×10^{-10}	-2.892×10^{-10}	1.7653	1.1032	0.31008	0.90617
10	Exponential	$C_t = a (b-\exp(-ct))$	a= 1.76 b= 28.75 c= -8.3822	a= 3.7172 b= 2.8908 c= 0.0012	0.159	0.001	-1.3657×10^{-12}	-0.002815	1.6188	1.3354	0.25895	1.2577
11	Logistic	$C_t = a / (1 + b \exp(-ct))$	a= 50.6 b= 0.036 c= -8.7351	a= 7.092 b= 0 c= 2.649	0.159	-8.9484×10^{-14}	9.8055×10^{-14}	-1.0962×10^{-11}	1.6188	1.3362	0.25895	1.2588
12	Two-term	$C_t = a \exp(-bt)+c \exp(-dt)$	a= 24.867 b= 0 c= 25.381 d= 0	a= 3.546 b= 0 c= 3.546 d= 0	-1.0911×10^{-9}	-3.4173×10^{-12}	-2.6178×10^{-8}	2.4369×10^{-6}	1.7653	1.3362	0.31008	1.2588
13	Diffusion	$C_t = a \exp(-bt) + (1-c) \exp(-cdt)$	a= 49.2498 b= 0 c= 0.0018 d= 0	a= 6.0967 b= 0 c= 0.0047 d= 0	-9.4229×10^{-12}	-4.3761×10^{-11}	4.8511×10^{-8}	-3.551×10^{-8}	1.7653	1.3362	0.31008	1.2588
14	Fourier	$C_t = a+b \cos(ct) + d \sin(ct)$	a= $3.55\times10^{+8}$ b= $-3.55\times10^{+8}$ c= 0 d= 18023.749	a= 23.2261 b= -14.6134 c= 0.0436 d= -10.0634	0.791	0.9998	-1.397×10^{-7}	-4.4409×10^{-15}	0.80789	0.016685	0.064636	2.09×10^{-4}

where a is the baseline level, b the initial rate of change, and *c* the nonlinear coefficient indicating curvature. As summarized in Table 11, the a parameter was higher in fortified samples, although the observed ΔE at day 0 was actually lower, likely reflecting the model's sensitivity to overall curve shape rather than the absolute initial value. The b coefficient was negative and larger in magnitude in fortified samples, indicating a more rapid initial decrease in ΔE. Meanwhile, the c parameter was significantly higher in the control, suggesting more pronounced nonlinear changes and a sharper increase in color variation over time.

These findings align with previous research where zero-order kinetic models were used to describe ΔE changes in sliced pumpkin during drying [40] and to predict storage stability of kiwifruit [41].

Table 11. Statistical comparison of the quadratic model constants for ΔE.

Constant	Control	Fortified	p-value
a	0.0096 (*b)	0.0163 (a)	0.002
b	-0.1328 (a)	-0.4506 (b)	<0.001
c	49.2743 (a)	8.6137 (b)	<0.001

*Values with different letters in each row indicates a significant difference at the 0.05 level, while values with the same letters are not significantly different.

4. Conclusions

The results of this study demonstrated that the quality attributes of protein bars fortified with *Spirulina platensis* and phycocyanin—including moisture, water activity, titratable acidity, peroxide value, and color difference (ΔE)—underwent significant changes during 28 days of storage. The direction and magnitude of these changes were influenced by the composition of the protein bars, oxidative reactions, moisture changes, and physicochemical interactions within the product matrix. Kinetic modeling revealed that the Diffusion model best described moisture changes, the Rational model was most suitable for water activity, the Gompertz model effectively captured acidity and peroxide kinetics, and the Quadratic model provided the best fit for color difference (ΔE). Identifying these models not only enhances our understanding of quality dynamics during storage but also enables more accurate prediction of product behavior under real storage conditions.

The incorporation of spirulina and phycocyanin, owing to their antioxidant and bioactive properties, played a meaningful role in stabilizing several quality attributes. Specifically, they contributed to slowing lipid oxidation, moderating color changes, and preserving the overall visual quality of the bars. These findings highlight the potential of these natural ingredients as effective and clean-label additives in protein-based functional foods.

Overall, the study provides a scientific basis for designing and producing protein bars with improved stability during storage. Food manufacturers can apply the proposed kinetic models to better estimate shelf life and optimize both formulation and storage conditions. For future research, it is recommended to investigate the influence of different storage temperatures, relative humidity levels, and packaging types on physicochemical and sensory stability. Extending kinetic evaluations to longer storage periods or accelerated storage tests would also deepen the understanding of product behavior. Furthermore, economic feasibility studies and comparative assessments of spirulina and phycocyanin against other natural additives could guide the development of more sustainable and consumer-friendly protein products.

Acknowledgments

The authors gratefully acknowledge Guilan Science and Technology Park for providing financial support for this study through the Creativity and Innovation Grant [Grant No. 1403/4564]. The authors also thank Giltaz Food Industries Co. (Langarud, Guilan, Iran) for supplying the raw materials used in this research.

References

[1] Jabeen, S., Huma, N., Sameen, A., & Zia, M. A. (2020). Formulation and characterization of protein-energy bars prepared by using dates, apricots, cheese and whey protein isolate. *Food Sci. Technol., 41,* 197–207. https://doi.org/10.1590/fst.12220

[2] Sithari, J., Chandrasiri, T., & Wijesekara, K. (n.d.). Formulation and characterization of nutrient bars using underutilized seeds: Semolina and jackfruit seeds. *Appl. Biosyst. Technol.,* 1.

[3] Fanari, F., Bonaldo, A., Mandrioli, M., Fontanillas, R., Badiani, A., & Chemat, F. (2023). Enhancing energy bars with microalgae: A study on nutritional, physicochemical and sensory properties. *J. Funct. Foods, 109,* 105768. https://doi.org/10.1016/j.jff.2023.105768

[4] Rajabi, F. (2017). *High protein bars based on whey proteins* (Master's thesis, Norwegian University of Life Sciences, Ås).

[5] Jiang, Z., Chen, Y., Zhang, L., Wang, L., Hu, S., & Xu, B. (2021). High-protein nutrition bars: Hardening mechanisms and anti-hardening methods during storage. *Food Control, 127,* 108127. https://doi.org/10.1016/j.foodcont.2021.108127

[6] Soliman, T. N., Ali, R. F. M., Mohamed, G. F., & Abo El-Naga, S. (2023). Effect of applying beetroot juice and functional vegetable oils in the preparation of high protein nutrition bars on its physicochemical, textural and sensorial properties. *Egypt. J. Chem., 66*(1), 1–14. https://doi.org/ 10.21608/ejchem.2022.156451.6773

[7] Zhu, H., Zhao, L., Liu, J., Liu, Y., & Li, W. (2023). Anti-hardening effect and mechanism of silkworm sericin peptide in high protein nutrition bars during early storage. *Food Chem., 407,* 135168. https://doi.org/10.1016/j.foodchem.2022.135168

[8] Dietrich, R. B., Clarke, K., Smith, J. P., & Thomas, M. (2025). Role of protein and lipid oxidation in hardening of high-protein bars during storage. *J. Food Sci., 90*(1), e17657. https://doi.org/10.1111/1750-3841.17663

[9] Caporgno, M. P., & Mathys, A. (2018). Trends in microalgae incorporation into innovative food products with potential health benefits. *Front. Nutr., 5,* 58. https://doi.org/10.3389/fnut.2018.00058

[10] Bortolini, D. G., Maciel, G. M., da Silva, R. P. F. F., Brugnari, T., Haminiuk, C. W. I., & Macedo, G. A. (2022). Functional properties of bioactive compounds from *Spirulina* spp.: Current status and future trends. *Food Chem. Mol. Sci., 5,* 100134. https://doi.org/10.1016/j.fochms.2022.100134

[11] Maddiboyina, B., Ranjith Kumar, R., Govindaraju, K., & Prasad, S. (2023). Food and drug industry applications of microalgae *Spirulina platensis*: A review. *J. Basic Microbiol., 63*(6), 573–583. https://doi.org/10.1002/jobm.202200704

[12] Grahl, S., Strack, M., Weinrich, R., Mörlein, D., & Busch, C. (2018). Consumer-oriented product development: The conceptualization of novel food products based on *Spirulina* (*Arthrospira platensis*) and resulting consumer expectations. *J. Food Qual., 2018,* 1919482. https://doi.org/10.1155/2018/1919482
[13] AlFadhly, N. K., Al-Khazaali, M. A., & Al-Juhaishi, H. J. (2022). Trends and technological advancements in the possible food applications of *Spirulina* and their health benefits: A review. *Molecules, 27*(17), 5584. https://doi.org/10.3390/molecules27175584
[14] Wang, Y., Zhang, H., Li, L., & Xu, Y. (2023). The nutritional value of *Spirulina* and utilization research. *Life Res., 6*(3), 15. https://doi.org/10.53388/LR20230015
[15] Gentscheva, G., Ivanov, I., & Mihaylova, D. (2023). Application of *Arthrospira platensis* for medicinal purposes and the food industry: A review of the literature. *Life, 13*(3), 845. https://doi.org/10.3390/life13030845
[16] de Morais, M. G., Vaz, B. S., de Morais, E. G., & Costa, J. A. V. (2018). Phycocyanin from microalgae: Properties, extraction and purification, with some recent applications. *Ind. Biotechnol., 14*(1), 30–37. https://doi.org/10.1089/ind.2017.0009
[17] Athiyappan, K. D., Routray, W., & Paramasivan, B. (2024). Phycocyanin from *Spirulina*: A comprehensive review on cultivation, extraction, purification, and its application in food and allied industries. *Food Human.,* 100235. https://doi.org/10.1016/j.foohum.2024.100235
[18] Mohammadi-Gouraji, E., Soleimanian-Zad, S., & Ghiaci, M. (2019). Phycocyanin-enriched yogurt and its antibacterial and physicochemical properties during 21 days of storage. *LWT, 102,* 230–236. https://doi.org/10.1016/j.lwt.2018.12.057
[19] Pourghasemian, P., Pourfarzad, A., & Babakhani, A. (2025). Optimization of a brown rice protein bar supplemented with *Spirulina* and phycocyanin: FTIR-based analysis of protein secondary structures and multivariate quality assessment. *Appl. Food Res.,* 101259. https://doi.org/10.1016/j.afres.2025.101259
[20] Sparkman, K., Joyner, H. S., & Smith, B. (2019). Understanding how high-protein bar formulations impact their mechanical and wear behaviors using response surface analysis. *J. Food Sci., 84*(8), 2209–2221. https://doi.org/10.1111/1750-3841.14707
[21] Talemi, F. P., Pourfarzad, A., & Gheibi, S. (2025). Synergistic effects of bee pollen and propolis extract on protein bar properties: A multivariate chemometric analysis. *Discov. Food, 5*(1), 1–29. https://doi.org/10.1007/s44187-025-00541-0
[22] Lucas, B. F., de Morais, M. G., Santos, T. D., & Costa, J. A. V. (2018). *Spirulina* for snack enrichment: Nutritional, physical and sensory evaluations. *LWT, 90,* 270–276. https://doi.org/ 10.1016/j.lwt.2017.12.032
[23] Sabovics, M., Straumite, E., & Galoburda, R. (2014). The influence of baking temperature on the quality of triticale bread. In: *Proceedings of the 9th Baltic Conf. Food Sci. Technol. FOODBALT 2014* (pp. 202–206).
[24] Okpala, C. O. R., Bono, G., & Abramo, A. (2016). Lipid oxidation kinetics of ozone-processed shrimp during iced storage using peroxide value measurements. *Food Biosci., 16,* 5–10. https://doi.org/10.1016/j.fbio.2016.07.005
[25] Hematian Sourki, A., Abbasi, S., & Mousavi, S. M. (2013). Optimization of alkaline extraction for dietary fiber of coffee silver skin and its effect on the quality and shelf life of Iranian Barbari bread. *Iran. J. Nutr. Sci. Food Technol., 8*(1), 11–22.
[26] Jovanov, P., Bjelanović, J., Stupar, A., Vučinić, T., & Savić, G. (2021). High-protein bar as a meal replacement in elite sports nutrition: A pilot study. *Foods, 10*(11), 2628. https://doi.org/10.3390/foods10112628
[27] Pourfarzad, A., & Habibi-Najafi, M. B. (2012). Optimization of a liquid improver for Barbari bread: Staling kinetics and relationship of texture with dough rheology and image characteristics. *J. Texture Stud., 43*(6), 484–493. https://doi.org/10.1111/j.1745-4603.2012.00362.x
[28] Lucas, B. F., de Morais, M. G., Santos, T. D., & Costa, J. A. V. (2019). Snack bars enriched with *Spirulina* for schoolchildren nutrition. *Food Sci. Technol., 40,* 146–152. https://doi.org/10.1590/fst.06719
[29] Ashaolu, T. J., Zhao, G., & Li, X. (2021). Phycocyanin, a super functional ingredient from algae: Properties, purification, characterization, and applications. *Int. J. Biol. Macromol., 193,* 2320–2331. https://doi.org/10.1016/j.ijbiomac.2021.11.064
[30] Bayram, I., & Decker, E. A. (2023). Underlying mechanisms of synergistic antioxidant interactions during lipid oxidation. *Trends Food Sci. Technol., 133,* 219–230. https://doi.org/10.1016/j.tifs.2023.02.003
[31] Tańska, M., Konopka, I., & Ruszkowska, M. (2017). Sensory, physico-chemical and water sorption properties of corn extrudates enriched with *Spirulina*. *Plant Foods Hum. Nutr., 72,* 250–257. https://doi.org/10.1007/s11130-017-0628-z
[32] Al-Baarri, A. N. M., Ando, Y., Kitamura, Y., Sasaki, M., & Ohta, H. (2023). Accelerated shelf life determination of corn snack bars. *Ital. J. Food Saf., 12*(4), 10718. https://doi.org/10.4081/ijfs.2023.10718
[33] Marcinkowska-Lesiak, M., Onopiuk, A., Stelmasiak, A., Szmaja, A., & Poltorak, A. (2018). The effect of different level of *Spirulina* powder on the chosen quality parameters of shortbread biscuits. *J. Food Process. Preserv., 42*(3), e13561. https://doi.org/10.1111/jfpp.13561
[34] Hussain, S. Z., Rani, S., Nazir, S., & Rafiq, S. (2019). Development of low glycemic index muffins using water chestnut and barley flour. *J. Food Process. Preserv., 43*(8), e14049. https://doi.org/10.1111/jfpp.14049
[35] Srisuk, N., & Jirasatid, S. (2023). Development of instant pumpkin-fingerroot drink powder and its shelf life modeling. *Life Sci. Environ. J., 24*(1), 161–182. https://doi.org/10.14456/lsej.2023.14
[36] Tireki, S., Sumnu, G., & Sahin, S. (2023). Investigation of average crosslink distance and physicochemical properties of gummy candy during storage: Effect of formulation and storage temperature. *Phys. Fluids, 35*(5), 057111. https://doi.org/10.1063/5.0146761
[37] Yang, S., Wang, J., Liu, C., Zhang, J., & Chen, Y. (2021). Evaluation of cooking performance, structural properties, storage stability and shelf life prediction of high-moisture wet starch noodles. *Food Chem., 357,* 129744. https://doi.org/10.1016/j.foodchem.2021.129744
[38] Manzocco, L., Calligaris, S., Panozzo, A., & Nicoli, M. C. (2020). Modeling the effect of the oxidation status of the ingredient oil on stability and shelf life of low-moisture bakery products: The case study of crackers. *Foods, 9*(6), 749. https://doi.org/10.3390/foods9060749
[39] Monji, Z. B., Babakhani, A., Pourfarzad, A., & Farhoosh, R. (2025). Effect of phycocyanin and butylated hydroxytoluene on the oxidative stability of safflower oil: A comprehensive kinetic investigation. *Eur. J. Lipid Sci. Technol., 127*(1), e202400010. https://doi.org/10.1002/ejlt.202400010
[40] Chikpah, S. K., Essilfie, G., & Nyarko, A. (2022). Colour change kinetics of pumpkin (*Cucurbita moschata*) slices

during convective air drying and bioactive compounds of the dried products. *J. Agric. Food Res., 10,* 100409. https://doi.org/10.1016/j.jafr.2022.100409
[41] Zhang, W., Guo, L., Liu, Y., & Wang, X. (2021). Kinetic models applied to quality change and shelf life prediction of kiwifruits. *LWT, 138,* 110610. https://doi.org/10.1016/j.lwt.2020.110610